A Three-Dimensional Numerical Simulation of CO_2 Gas Bubble Transport at Anode in PEM Based Electrochemical Methanol Reformer

Yasodhar Surabattula , R. Balaji *, K.Ramya,

Centre for Fuel Cell Technology,
International Advanced Research Centre for Powder Metallurgy and New Materials (ARCI), IITM Research Park, Chennai, 600113, India
*Corresponding author Email: rbalaji@arci.res.in (R. Balaji).

Abstract

The accumulation of generated carbon dioxide(CO_2) gas bubbles at the anode flow channels during the operation of PEM based Electrochemical Methanol Reformer (ECMR) may influence the diffusion of reactants to reach its electrocatalytic sites and its performance. Hence, it is imperative to understand the gas-liquid interaction at the anode side of the ECMR. For the first time in the literature, we are reporting a 3D, unsteady, turbulent VOF model on aqueous methanol electrolyzer. In this study, numerical simulation of two-phase flow in the PEM based ECMR is studied to understand the CO_2 gas transportation at the flow channels using volume of fluid (VOF) method. We have considered two conventional flow channel types, namely parallel flow channel (PFC) and serpentine flow channel (SFC). Results show that serpentine flow channels are better in terms of effective gas removal at different operating current densities. The simulation results obtained in this study are compared with the experimental results available in the literature, and they are in good agreement with each other. The influence of liquid feed rate and contact angle on the serpentine flow channel are also studied. The simulation results show that the VOF method, along with the modelling strategy employed in this study, can be used to simulate the gas-liquid interactions even under turbulent conditions for different flow channels of the ECMR cell.

Keywords: *Hydrogen, Electrolyzer, Computational fluid dynamics (CFD), lectro Chemical Methanol reformer, Volume of fluids (VOF)*

1. Introduction

Hydrogen is considered as a clean energy carrier, which can be produced from various methods like steam reforming of natural gas, biogas fermentation, and water electrolysis. A significant portion of the hydrogen in the globe is produced by steam reformation of hydrocarbons and gasification of coal[1,2]. The 'cleanest way' to produce on-site hydrogen is electrolysis of water, if coupled with the electricity derived from renewable sources like solar energy, wind energy. Proton exchange membrane (PEM) based electrolysis is one of the advanced technologies which can offer pure hydrogen production with modular designs and high efficiency. It is well known that the practical PEM water electrolysis consumes about more than 5.0 kWhr of energy to produce per cubic meter of hydrogen, which makes this process economically unattractive except in niche areas.

PEM based Electrochemical Methanol Reformation (ECMR) is a method that combines aspects of both the processes of electrolysis and reformation. If the required electrical potential is supplied across two electrodes separated by a solid electrolyte, high pure hydrogen can be produced. The energy required to harvest the same amount of hydrogen is less than the PEM based water electrolysis [3–5]. The hydrogen produced from this process is free from carbon dioxide and carbon monoxide. This method comes with the advantage of the elimination of the external purification system, usually employed in the reformation process.

Figure1 describes the components and function of PEM based ECMR cell. During DC power is supplied, aqueous methanol is circulated at the anode side of the cell, and it produces CO_2 at the anode, and hydrogen gas is evolved at the cathode. The electrochemical reactions at electrodes can be expressed as

Anodic reaction : $CH_3OH + H_2O \rightarrow CO_2 + 6H^+ + 6e^-$ (1)

Cathodic reaction : $6H^+ + 6e^- \rightarrow 3H_2$ (2)

Overall reaction : $CH_3OH + H_20 \rightarrow CO_2 + 3H_2$ (3)

The anodic reaction taking place at ECMR is similar to that of the anodic reaction of the Direct Methanol Fuel cell (DMFC). The performance of ECMR also depends on the effective removal of produced CO_2 bubbles from the anode outlet. Otherwise, it could choke the flow channel of aqueous methanol and increase the fuel concentration gradient along the flow channel and may hinder the electrochemical reaction. Hence, studying the interaction between aqueous methanol and carbon dioxide is very important while designing of the electrolyzer flow field plate pattern in a way to minimize the mass transport issues on the anode side of the ECMR cell.

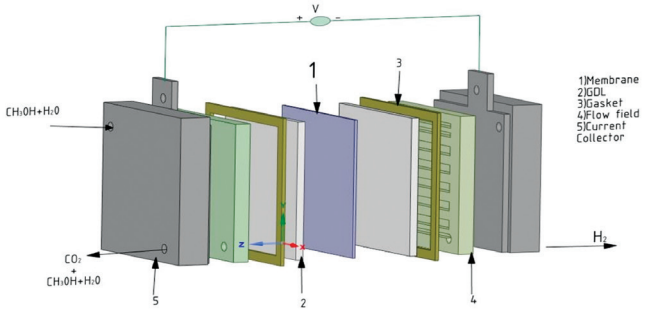


Fig. 1. Schematic of methanol-water solution electrolysis

In the literature, various studies have been carried out to understand the liquid and gas interaction in PEM based fuel cell system using advanced techniques like X-ray radiography, Particle image velocimetry (PIV) [6–9]. Yang et al. studied the influence of different flow field designs on the DMFC performance using a transparent cell setup. They observed that the DMFCs designed with the single serpentine flow fields (SSFF) resulted in improved performance than those with the Parallel flow fields (PFF). They also reported the channel blockages by produced CO_2 gas bubbles in the PFFs, at high currents and low liquid feed rate; however, this phenomenon was not observed in the SSFF [10]. T. Hutzenlaub et al. reported the influence of wetting properties on the bubble dynamics of DMFC. They compared hydrophobic and hydrophilic flow channels; they found a low-pressure drop in the case of hydrophilic flow channels. The critical fuel velocity to detach the bubble depends on the bubble length [11]. Yuan.W et al. experimentally examined the behavior of two-phase flow dynamics with temperature on the anode side of DMFC using a transparent cell. Further, in the case of PEM based water electrolyzer, the two-phase flow phenomena were studied in the literature using above similar techniques like optical characterization, X-ray radiography, neutron tomography [12–17].

Furthermore, the various computational techniques have also been employed to study the water-gas dynamics in PEM based system. To illustrate the interface dynamics and bubble visualization, techniques such as the pore - network (PN), the level set (LS) and the Volume of fluids (VOF) methods are used. In this, The VOF method is widely used in PEM fuel cells/water electrolyzer to study liquid-gas interaction [16-21]. Kang et al. [20] successfully simulated bubble generation in a 'T' junction channel using VOF methods and found that, high liquid viscosities resulted in the small bubble slugs along the channel, this could be due to the stronger shear force from the fluid. They have also validated with experimental results. Kang et al. [21] also employed the VOF method to track, the gas-liquid interface in parallel channels of DMFC considering flow type as laminar with the limited active area of 96 sq.mm. Shu yuan et.al studied the bubble evolution and transport processes as well as the mechanisms of how bubbles impact the PEMWE Performance [22]. The micro Gas bubble dynamics and two-phase flow are visualised by in-situ high-speed camera coupled with a specific design in PEM based water electrolyser [23].

The above literture study shows the significance of flow field designs and interaction of gas and liquid within the cell on the performance of PEM based

fuel cell/electrolyzer. However, in the case of the PEM based ECMR cell, the electrodes are porous in nature and flow type, which occurs within the cell would be turbulence in nature. Hence, this methodology should be validated for larger active areas and un-study turbulent flows that develop at the outlet. In the present study, we have adopted a similar methodology as proposed by Kang et al. [21], to study the bubble generation in ECMR for a larger area of 900 sq.mm with two different flow channels (parallel and serpentine design) using 3D unsteady, and turbulent flow conditions. Simulation results are compared with experimental results from literature published by Yuan et al [24].

2. Numerical model description

2.1. Volume of Fluid (VOF) method

VOF is proposed by Hirt C.W [25], which is suitable for simulation of immiscible fluids and provides the information between the interface of the mixture's phases, for example, the fraction of gas as shown in Fig.2. In the present study, it has been employed to track the gas-liquid interface at anode side of ECMR cell and investigate the bubble behavior within the flow channel.

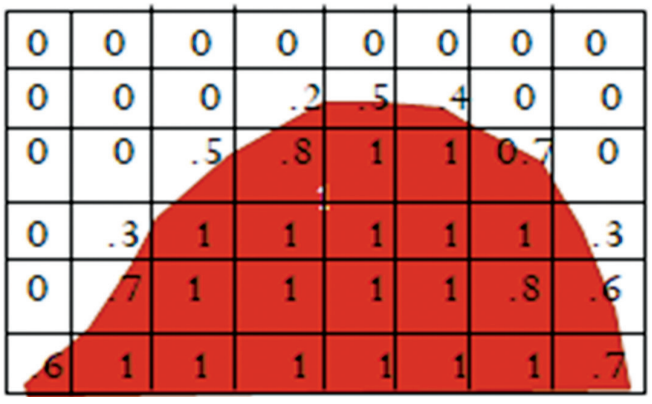


Fig. 2. Fraction of volume of the fluid

2.2. Multiphase flows in ECMR

Similar to the other PEM based systems, understanding of multiphase flow phenomena in ECMR is crucial for better design of the cell to improve performance and efficiency. Initially, an attempt has been made to study the interaction between supplied aqueous methanol (liquid) and generated carbon dioxide (gas) and its removal efficiency under various feed rate of reactant. In ECMR cell, aqueous methanol is supplied through the flow channels and diffuses into the gas diffusion layer (GDL) and reaches the electrocatalyst layer (CL). The evolved carbon dioxide at the electrocatalyst layer diffuses back into the flow channel through the GDL, flowing against the fresh feed aqueous methanol. This gas-liquid interaction causes a two-phase flow scenario in the ECMR. The VOF method is employed in this study to simulate the bubble generation inside the flow channels of the reactant distribution plate.

2.3. Computational domain description

The ECMR anode is consisted by flow field channels and a porous electrode layer. In this uniform porous electrode layer contains 0.1mm thick catalyst layer (CL) on top of the 0.3mm gas diffusion layer (GDL), which is directly linked with the flow channel, as shown in Figure 3.

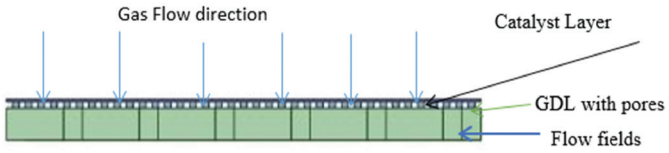


Fig. 3. A schematic describing different parts of the domain

The entire GDL consist of square holes (0.4mm × 0.4mm) and its spacing between adjacent holes is maintained as 1 mm from its middle point. Figure 4 shows the domains of the serpentine and parallel flow channel used in this study. There are thirteen serpentine flow channels in the entire active area of 900 sq.mm, which has 1.2 mm width and 1.5mm depth per channel, rib width, and other geometric details of flow channels are listed in Table 1.

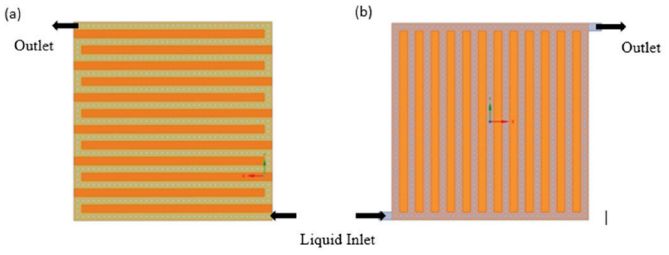


Fig. 4. (a) Serpentine flow channel (b) Parallel flow channel flow domains used in study

Table 1: Geometric parameters of two flow field patterns

Parameters	Serpentine	Parallel	Units
Effective area	900	900	mm^2
Channel width	1.2	1.2	mm
Channel depth	1.5	1.5	mm
Channel length	39	3	mm
Rib width (mm)	1.2	1.2	mm

3. Mathematical Model

In the present study, FLUENT 19.1 is used to simulate the two-phase, unsteady and three-dimensional flows with the VOF method. The VOF tracks interface between gas and liquid by solving the continuity equation for the volume fraction in individual cells for one of the phase q. and its equation can be expressed as follow:

$$\frac{\partial(\alpha_q\rho_q)}{\partial t} + \nabla\cdot(\alpha_q\rho_q\vec{v}_q) = 0 \quad (4)$$

Here α_q is the volume fraction of the fluid q in a cell. The pressure jump is considered across the interface; the velocity field is considered as continuous. The equation for conservation of mass eq.5 and momentum eq.6 are expressed as follow:

$$\frac{\partial\rho}{\partial t} + \nabla\cdot\rho\vec{v} = 0 \quad (5)$$

$$\frac{\partial(\rho\vec{v})}{\partial t} + \nabla\cdot(\rho\vec{v}\vec{v}) = \nabla p + \nabla\cdot[\mu(\nabla\vec{v} + \nabla\vec{v}^T)] + \rho\vec{g} + \vec{F} \quad (6)$$

Here ρ is density, $\vec{v}$ is velocity and, p is static pressure, and μ is dynamic viscosity.

The density and viscosity in the above equations are calculated by using the following equations for two fluids with densities (ρ_1, ρ_2) and viscosities (μ_1,μ_2)

$$\rho = \alpha_2\,\rho_2 + (1-\alpha_2)\rho_1 \quad (7)$$

$$\mu = \alpha_2\,\mu_2 + (1-\alpha_2)\mu_1 \quad (8)$$

Turbulence: we have considered Menter's Shear Stress Transport (SST) [26] to account the flow turbulence which develops at the outlet,

$$\nabla\cdot\left(\rho\vec{v}k - \left(\mu + \frac{\mu_t}{\sigma_k}\right)\nabla k\right) = P_k - \beta^*\rho k\omega + P_{kb} \quad (9)$$

$$\nabla\cdot\left(\rho\vec{v}\omega - \left(\mu + \frac{\mu_t}{\sigma_t}\right)\nabla\omega\right) = \alpha\frac{\omega}{k}P_k - \beta\rho k\omega^2 + P_{\omega b} \quad (10)$$

The more details of the above equations can be found in [19,26].

3.1. Boundary conditions and initial conditions

In the present two-phase simulation, 2.0 M methanol solution is considered as liquid and carbon dioxide is considered as a gas with its properties as listed in Table 2 from the literature [13].

Table 2: Properties of the primary and secondary fluids

Phase	Density(kg/m^3)	Viscosity (Pa s)
Primary phase(liquid)	988	0.001212
Secondary phase(gas)	1.7878	$1.37e^{-5}$

Multiphase model, surface tension model, formulation, and other parameters are listed in Table 3. Table 4 and Table 5 describes the boundary conditions in different cases. The production rate of carbon dioxide gas is proportional to the operating current density of the electrolyzer. The operating current density is of ECMR is converted into gas inlet velocity at the electrode according the faradays law. The molar flow rate is calculated using the equation 11 and then converted into gas-velocity.

$$\frac{dN}{dt} = \frac{i}{nF} \quad (11)$$

Where i is current density and n is number of electrons and F is the Faraday constant (96,485 C per mole of electron)

Assumptions

In order to reduce the complexity involved during solving governing equations, the following few assumptions are considered. Since the complete 3D numerical modelling of electrolyzer are a highly time consuming and computationally very expensive process.

- Transient flows at isothermal conditions (Room Temperature) are considered, without any electrochemical reactions.
- Crossover of methanol solution from anode to the cathode through the membrane is neglected.
- The generation of CO_2 gas on the surface of the catalyst layer is assumed to be uniform.
- Produced CO_2 gas diffuses through the porous gas diffusion layer and enters into the flow channel.

- The concentration of aqueous methanol is considered uniform across the flow channels.
- Fluids are considered as incompressible and ideal.

3.2. Numerical setup

Table 3 contains the numerical schemes used in this study. The time step size(s) is set at $1x10^{-4}$ S, whereas the total number of time steps is taken as 5000, the simulation time in each case equals to 0.5 seconds. The contact angle between the flow field plate substrate and reactant is set at 120°.

Table 3 List of Models and parameters employed in this study

Parameter	Model/Value
Multiphase model	VOF
Volume of fraction cut-off	1e-06
Interface modelling type	Sharp
Flow type	Turbulent
Surface tension model	Continuum surface force
Formulation	Implicit
Pressure-Velocity coupling scheme	PISO
Wall adhesion	Enabled
Contact angle	120°

Initially, the influence of cell operating current density on gas bubble behaviour was studied with the flow field plate having serpentine and parallel flow channels at the condition listed in Table 4. Further, the influence of the liquid feed rate and contact angle was also studied with the serpentine flow channel at different conditions, as listed in Table 5. To validate the results, the Isosurfaces of gas volume fraction (0.001) at time 0.5 s are compared with the results obtained from experimental visualization studies in the literature [24].

Table 4 Boundary and initial conditions for cases 1, 2 and 3

Case No	Liquid feed rate (ml min^{-1})	Liquid-inlet velocity (m s^{-1})	Current density (mA cm^{-2})	Gas inlet velocity (m s^{-1})
1	1	$9.259x10^{-3}$	20	$1.25x10^{-5}$
2	1	$9.259x10^{-3}$	60	$3.75x10^{-5}$
3	1	$9.259x10^{-3}$	100	$6.25x10^{-5}$

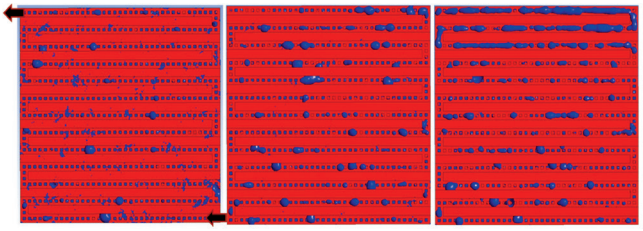
Table 5: Boundary conditions and initial conditions for cases A, B, C and D

Case No.	Liquid feed rate (ml min^{-1})	Liquid-inlet velocity (m s^{-1})	Current density (mA cm^{-2})	Gas inlet velocity (m s^{-1})
A	0.1	$9.259x10^{-4}$	80	$5x10^{-5}$
B	0.3	$2.777x10^{-3}$	80	$5x10^{-5}$
C	0.6	$5.555x10^{-3}$	80	$5x10^{-5}$
D	0.8	$7.407x10^{-3}$	80	$5x10^{-5}$

4. Results and discussions

4.1. Effect of Current density on gas bubble behaviour

The influence of applied current density on the flow of gas bubbles distribution in serpentine flow channels is studied. From the figure 5, it can be observed that fewer gas bubbles are formed at a lower current density of 20 mA/cm^2 and a further increase in current density to 60 mA/cm^2, the generated CO_2 gas bubbles are travels through porous electrode layer to reach its flow channel. At some places, it is also observed the smaller gas bubbles are merged and forming larger bubbles, especially towards at the outlet of the flow channel**.** At the higher current density operation (100 mA/cm^2), large size gas bubbles are observed in the channels. The coalesce of small bubbles turned into big gas slug towards the outlet of the channel, which may result in poor supply for fresh reactant. The above-observed results are in decent pact with experimental visualization results obtained by Wei Yuan et al. for DMFC[24].



(a) 20 mA/cm-2 (b) 60 mA/cm-2 (c) 100mA/cm-2

Fig.5. Simulation results on Gas bubble behaviour in serpentine flow channel

Figure 6. Shows the gas bubbles distribution pattern observed at different current density with a serpentine flow channel. The above similar gas bubble distribution pattern was observed up to 60 mA/cm^2 forming smaller gas slugs in the

channels. It is increased drastically while operating at 100mA/cm^2, which is comparatively higher than the distribution behaviour observed with the parallel flow channel. Further, it is also observed that the distribution of gas slugs is higher only at last two channels in the case of the serpentine flow channel, but in the parallel flow channel, the slugs are distributed almost at entire flow channels area, which leads blocking effect of reactant resulting lower performance of the electrolyzer.

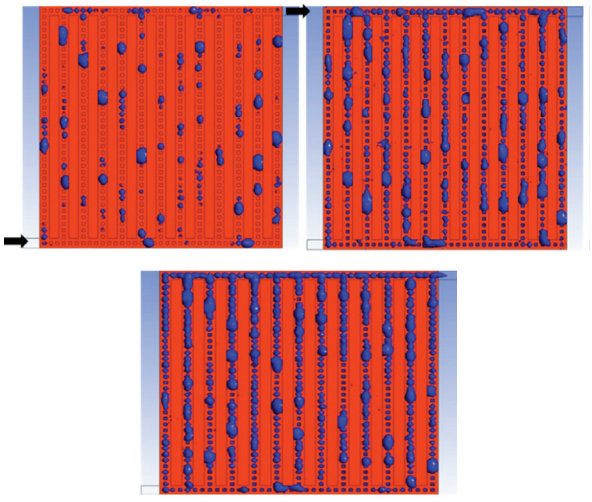
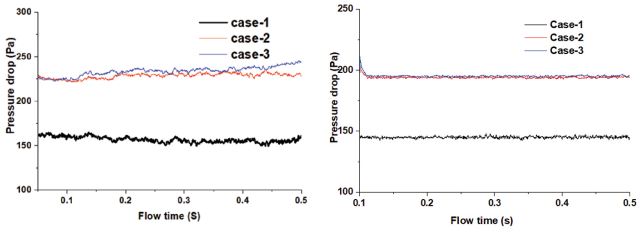


Fig. 6. Simulation results on gas bubble behaviour in parallel flow channel

The pressure drop characteristics of the flow field pattern were studied and results are presented in figure 7. The higher-pressure drop is observed for serpentine flow channel pattern when compared to parallel flow channel pattern and it may be attributed to the right angel corner nature of the serpentine pattern. The increase in current density results in large gas slugs on the channel, which are responsible for the increase in flow resistance creating a high pressure drop in each case. Hence further study on the influence of flow rate of reactant and contact angle on gas bubble distribution was confined only with the serpentine flow channel pattern.



(a) 20 mA/cm^2 (b) 60 mA/cm^2 (c) 100mA/cm^2

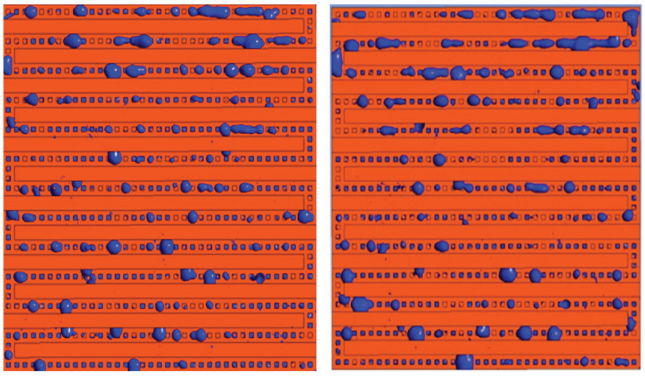
Fig. 7. Pressure difference between the outlet and the inlet of (a) Serpentine and (b) parallel flow channel for various cases.

4.2. Effect of reactant feed rate on gas bubble behaviour

The influence of reactant feed rate on gas bubbles distribution behaviour at the current density of 80 mA/cm^2 was studied and the results are shown in figure 8. The feed rate was varied up to 0.8 ml/min to ascertain its effect on gas bubble growth and evolvement precisely. The smaller gas bubbles are formed and attached to the walls of the flow channel at 0.1 ml/min. Further increase in flow rate at 0.3 ml/min the shape of the CO_2 gas bubbles is changed and moves away from the wall surface due to an increase in force created by the liquid flow. Upon further increase in liquid feed rate to 0.8 ml/min, it helps in effective removal of gas by forming a gas slug resulting in more areas can be exposed for methanol transportation for electrochemical reaction. It will increase the mass transfer efficiency while operating electrolyzer.

The pressure drops observed at different reactant feed rates (shown in fig 9) in different cases, as listed in table 5. The pressure drops increases with increasing feed rate and it may be attributed to the increase in flow velocity at higher feed rate resulting in the formation of gas slug.

In the Case-A, the flow rate is very less and low-pressure drop is observed, when the flow rate is increased the increase in flow velocity causes the gas bubbles to form a gas slug, the formation of slug results in higher pressure drop.



0.1 ml/min 0.3 ml/min

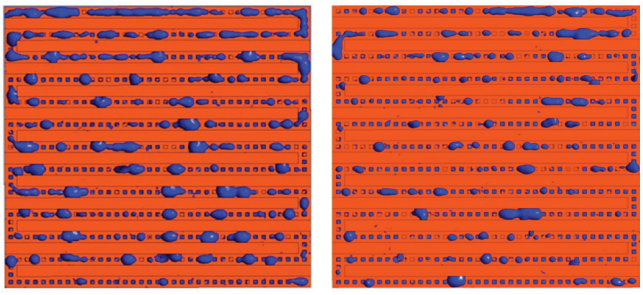


Fig.8 Gas bubble behaviour in serpentine flow channel at various flow rates

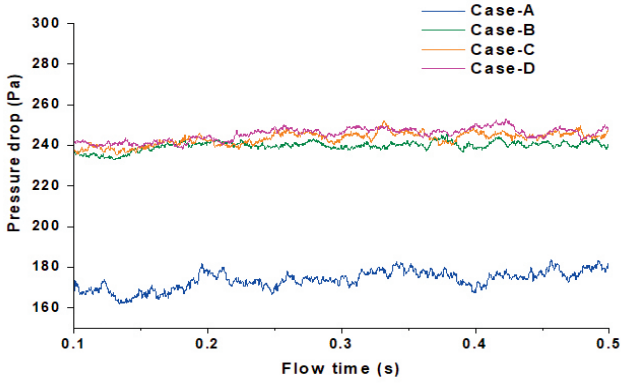


Fig. 9. Pressure drop in the Serpentine flow channel for various cases, as listed in Table 5.

4.3. Influence of contact angle on gas bubble behaviour

It is very essential to study the influence of the bipolar plate surface's nature on the performance of the electrolyzer. Bipolar plates can be made up of different materials; the contact angles of these bipolar plates may fall between the hydrophobic and hydrophilic regions. To understand the effect of contact angle on the gas-dynamics, three different contact angles, 70°, 90°, and 120°, are considered for the studies with the serpentine flow channel. The applied current density and reactant feed rate were considered as 100 mA cm^{-2} and 1 ml/min, respectively. Figure.10 shows that the increase in contact angle results in a more sluggish flow of gas bubbles. The bubble formation process can be identified into three distinct stages termed (1) nucleation stage, (2) growth stage, and (3) detachment stage The influence of contact angle on each stage of bubble formation are important by analysing the evolution of interface equilibrium and force balance conditions [27]. The bubble size increases with increasing contact angle and the nucleation stage becomes negligible compared to the other two stages. That's because with the contact angle increasing, the growth stage is more dominant compared to the nucleation stage inducing the smaller gas bubbles to coalesce and form gas slugs near the outlet of the serpentine flow channel, as shown in the Fig.10(C). Further, it also increases the pressure drop on the more hydrophobic surface, as seen in Figure 11.

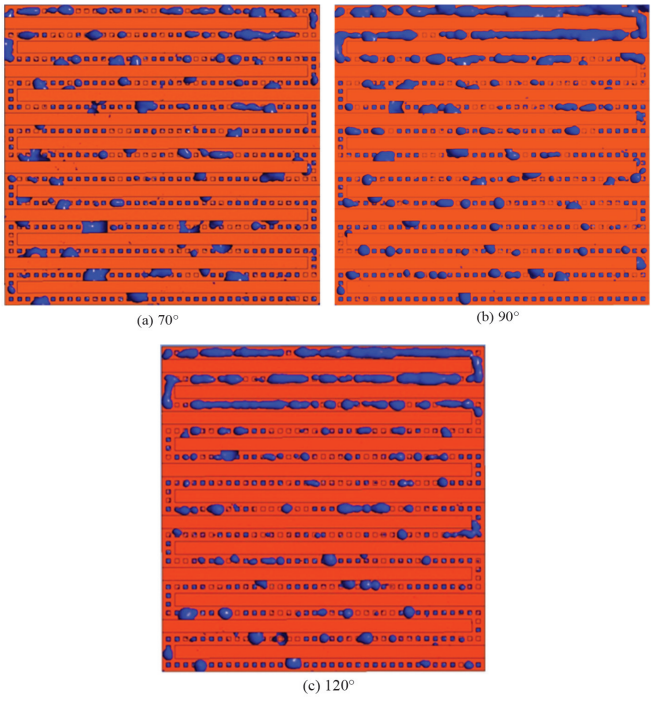


Fig.10 The effect of gas bubble behaviour in a serpentine flow channel under different contact angles with the wall surface

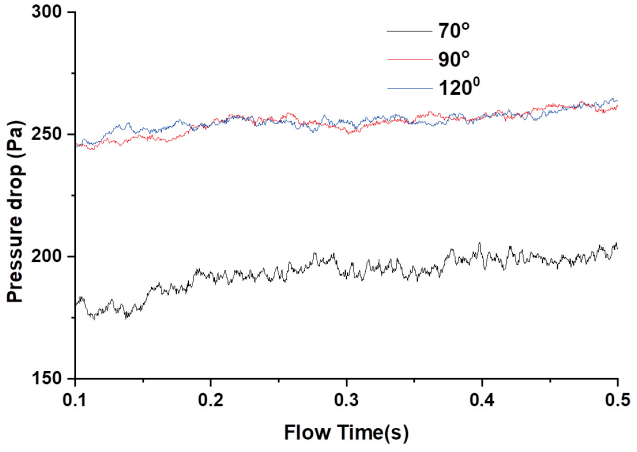


Fig. 11. Pressure drop in the Serpentine flow channel under different contact angles with the wall surface.

5. Conclusions

In the present study, the interaction of feed aqueous methanol and evolved Carbon dioxide (gas)-in PEM based ECMR cell was analysed using three dimensional, transient, turbulent VOF model employing Fluent 19.1 software. In order to reduce the complexity of the modelling, the electrochemical reactions are neglected and only the anode side gas-liquid interactions in the porous electrode layer and flow channels are considered. The influence of applied current density is studied in two different flow channel patterns (serpentine and parallel). Further, the effect of aqueous methanol feed rate and contact angle on the serpentine flow channel is also simulated and the important findings of this study are summarised below:

- In both parallel and serpentine designs, the pressure drops (inlet to outlet) increases with an increase in applied current density (i.e., the rate of production of carbon dioxide gas).
- At higher current densities (i.e., at case -2 and case-3), larger gas bubbles are observed across the channels on the parallel flow channel design, whereas in the case of serpentine design, large gas slugs are seen only at the channels near to the outlet.
- The comparative study between serpentine and parallel flow channels confirms that serpentine flow channel design performs better in terms of the removal of CO_2 bubbles from the porous surface of the electrode effectively.
- The effective removal of carbon dioxide gas bubbles is seen at a higher contact angle between the flow field plate substrate and feed reactant at the expense of a higher pressure drop.

This numerical study is aimed to understand the gas bubble and liquid interaction in PEM based ECMR cell and detailed numerical model, which can predict the entire performance of the ECMR cell are underway and would be published in the future.

Acknowledgement

The authors would like to thank The Director, ARCI, for his constant support and encouragement and the Department of Science and Technology, Government of India, for financial assistance. Yasodhar Surabattula thanks ARCI for the ARCI fellowship under which this work was carried out.

References

[1] M. Carmo, D.L. Fritz, J. Mergel, D. Stolten, A comprehensive review on PEM water electrolysis, Int. J. Hydrogen Energy. 38 (2013) 4901–4934. https://doi.org/10.1016/j.ijhydene.2013.01.151.

[2] H. Ju, S. Badwal, S. Giddey, A comprehensive review of carbon and hydrocarbon assisted water electrolysis for hydrogen production, Appl. Energy. 231 (2018) 502–533. https://doi.org/10.1016/J.APENERGY.2018.09.125.

[3] D.Gang, S.Park, J.Min Yoo, M.Gu, Electrochemical Reforming of Methanol using Multilayer Nanoarchitectonics with Ligand Exchange-Induced Layer-by-Layer Assembly toward Electrocatalytic Hydrogen Production. *ACS Appl. Energy Mater.* 7, 10, (2024) 4572–4580.

https://doi.org/10.1021/acsaem.4c00653

[4] N Manjula, R Balaji, K Ramya, N Rajalakshmi., Hydrogen production by electrochemical methanol reformation using alkaline anion exchange membrane based cell Int. J.Hydrogen Energy 45 (17), (2020) 10304-10312.

https://doi.org/10.1016/j.ijhydene.2019.08.202

[5] S.Menia, H.Tebibel, F.Lassouane, A.Khellaf ,I.Nouicer, Hydrogen production by methanol aqueous electrolysis using photovoltaic energy: Algerian potential, Int. J.Hydrogen Energy 42 , (2017) 8661-8669

https://doi.org/10.1016/j.ijhydene.2016.11.178

[6] A. Bazylak, Liquid water visualization in PEM fuel cells: A review, Int. J. Hydrogen Energy. 34 (2009) 3845–3857. https://doi.org/10.1016/J.IJHYDENE.2009.02.084.

[7] Z.W. Dunbar, R.I. Masel, Magnetic resonance imaging investigation of water accumulation and transport in graphite flow fields in a

polymer electrolyte membrane fuel cell: Do defects control transport?, J. Power Sources. 182 (2008) 76–82. https://doi.org/10.1016/J.JPOWSOUR.2008.03.057.

[8] J. Lee, J. Hinebaugh, A. Bazylak, Synchrotron X-ray radiographic investigations of liquid water transport behavior in a PEMFC with MPL-coated GDLs, J. Power Sources. 227 (2013) 123–130. https://doi.org/10.1016/J.JPOWSOUR.2012.11.006.

[9] S.-G. Kim, S.-J. Lee, A review on experimental evaluation of water management in a polymer electrolyte fuel cell using X-ray imaging technique, J. Power Sources. 230 (2013) 101–108. https://doi.org/10.1016/J.JPOWSOUR.2012.12.030.

[10] H. Yang, T.S. Zhao, Effect of anode flow field design on the performance of liquid feed direct methanol fuel cells, Electrochim. Acta. 50 (2005) 3243–3252. https://doi.org/10.1016/j.electacta.2004.11.060.

[11] T. Hutzenlaub, N. Paust, R. Zengerle, C. Ziegler, The effect of wetting properties on bubble dynamics and fuel distribution in the flow field of direct methanol fuel cells, J. Power Sources. 196 (2011) 8048–8056. https://doi.org/10.1016/j.jpowsour.2011.05.070.

[12] I. Dedigama, P. Angeli, N. van Dijk, J. Millichamp, D. Tsaoulidis, P.R. Shearing, D.J.L. Brett, Current density mapping and optical flow visualisation of a polymer electrolyte membrane water electrolyser, J. Power Sources. 265 (2014) 97–103. https://doi.org/10.1016/J.JPOWSOUR.2014.04.120.

[13] S. Sadeghi Lafmejani, A.C. Olesen, S.K. Kaer, Analysing Gas-Liquid Flow in PEM Electrolyser Micro-Channels, ECS Trans. 75 (2016) 1121-1127. https://doi.org/10.1149/07514.1121ecst.

[14] O.F. Selamet, U. Pasaogullari, D. Spernjak, D.S. Hussey, D.L. Jacobson, M.D. Mat, Two-phase flow in a proton exchange membrane electrolyzer visualized in situ by simultaneous neutron radiography and optical imaging, Int. J. Hydrogen Energy. 38 (2013) 5823-5835. https://doi.org/10.1016/j.ijhydene.2013.02.087.

[15] M.A. Hoeh, T. Arlt, N. Kardjilov, I. Manke, J. Banhart, D.L. Fritz, J. Ehlert, W. Luke, W. Lehnert, In-Operando Neutron Radiography Studies of Polymer Electrolyte Membrane Water Electrolyzers, ECS Trans. 69 (2015) 1135-1140.

https://doi.org/10.1149/06917.1135ecst.

[16] M.A. Hoeh, T. Arlt, I. Manke, J. Banhart, D.L. Fritz, W. Maier, W. Lehnert, In operando synchrotron X-ray radiography studies of polymer electrolyte membrane water electrolyzers, Electrochem. Commun. 55 (2015) 55-59. https://doi.org/10.1016/j.elecom.2015.03.009.

[17] J.O. Majasan, J.I.S. Cho, I. Dedigama, D. Tsaoulidis, P. Shearing, D.J.L. Brett, Two-phase flow behaviour and performance of polymer electrolyte membrane electrolysers : Electrochemical and optical characterisation, Int. J. Hydrogen Energy. 43 (2018) 15659–15672. https://doi.org/10.1016/j.ijhydene.2018.07.003.

[18] P. V Suresh, S. Jayanti, Effect of air flow on liquid water transport through a hydrophobic gas diffusion layer of a polymer electrolyte membrane fuel cell, Int. J. Hydrogen Energy. 35 (2010) 6872–6886. https://doi.org/10.1016/j.ijhydene.2010.04.052.

[19] R.B. Ferreira, D.S. Falc, Numerical simulations of two-phase fl ow in proton exchange membrane fuel cells using the volume of fl uid method - A review, J. Power Sources 277 (2015) 329–342

[20] S. Kang, B. Zhou, Numerical study of bubble generation and transport in a serpentine channel with a T-junction, Int. J. Hydrogen Energy. 39 (2014) 2325–2333. https://doi.org/10.1016/j.ijhydene.2013.11.115.

[21] S. Kang, B. Zhou, M. Jiang, Bubble behaviors in direct methanol fuel cell anode with parallel design, Int. J. Hydrogen Energy. 42 (2017) 20201–20215. https://doi.org/10.1016/j.ijhydene.2017.06.149.

[22] S. Yuan, Zhao, X.Cai, L. An, S.Shen, X.Yan J. Zhang, Bubble evolution and transport in PEM water electrolysis: Mechanism, impact, and management. Progress in Energy and Combustion Science 96 (2023) 101075,1-36.

https://doi.org/10.1016/j.pecs.2023.101075

[23] Y.Li, Z.Kang, J.Mo, G.Yang, S. Yu,D.A. Talley, Bo Han, F.Zhang In-situ investigation of bubble dynamics and two- phase flow in proton exchange membraneelectrolyzer cells. Int.J.Hydrogen Energy 43(2018) 11223-11233.

https://doi.org/10.1016/j.ijhydene.2018.05.006

[24] W. Yuan, A. Wang, Z. Yan, Z. Tan, Y. Tang, H. Xia, Visualization of two-phase flow and temperature characteristics of an active liquid-feed direct methanol fuel cell with diverse flow fields, Appl. Energy. 179 (2016) 85–98. https://doi.org/10.1016/j.apenergy.2016.06.127.

[25] C. W. Hirt, B. D. Nichols, Volume of Fluid (VOF) Method for the Dynamics of Free Boundaries*, J. Comput. Phys. 39 (1981) 201–225. https://doi.org/10.1007/s40998-018-0069-1.

[26] F.R. Menter, Two-equation eddy-viscosity turbulence models for engineering applications, AIAA J. 32 (1994) 1598–1605. https://doi.org/10.2514/3.12149

[27] J.Yuan, Y.Li ,Y.Zhou, “Effect of contact angle on bubble formation at submerged orifices.J Mater Sci 49 (2014) 8084–8094.

https://DOI 10.1007/s10853-014-8516-5